Environmental Science & Technology

pubs.acs.org/est

Article

Importance of Attachment Efficiency in Determining the Fate of PS and PVC Nanoplastic Heteroaggregation with Natural Colloids Using a Multimedia Model

Fazel Abdolahpur Monikh,* Joris T. K. Quik, Mark R. Wiesner, Andrea Tapparo, Paolo Pastore, Hans-Peter Grossart, Jarkko Akkanen, Raine Kortet, and Jussi V.K. Kukkonen

Cite This: *Environ. Sci. Technol.* 2025, 59, 4674−4683

Read Online

ACCESS | Metrics & More | Article Recommendations | Supporting Information

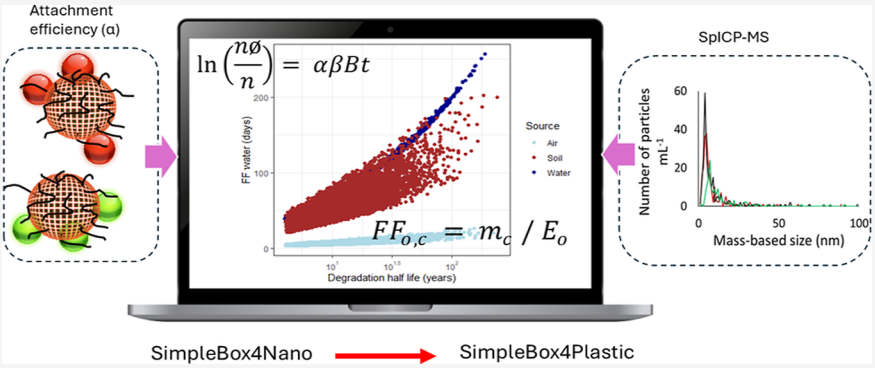

ABSTRACT: Here, we assessed the heteroaggregation of polystyrene (PS) and poly(vinyl chloride) (PVC) nanoplastics with SiO_2 as a model of natural colloids. Homoaggregation and heteroaggregation were evaluated as a function of $CaCl_2$ (0−100 mM) and natural organic matter (NOM) (50 mg L^{-1}) at a designated concentration of nanoplastics (200 μg L^{-1}). Critical coagulation concentrations (CCC) of nanoplastics were determined in homoaggregation and heteroaggregation experiments with SiO_2 and $CaCl_2$. The attachment efficiency (α) was calculated by quantifying the number of nanoplastics in the presence of $CaCl_2$, NOM, and SiO_2 using single-particle inductively coupled plasma mass spectrometry (spICP-MS) and pseudo-first-order kinetics. The calculated α was fed into the SimpleBox4Plastics model to predict the fate of nanoplastics across air, water, soil, and sediment compartments. Nanoplastics exhibited high stability against homoaggregation, while significant heteroaggregation with SiO_2 occurred at $CaCl_2$ concentrations above 100 mM. The influence of NOM was also evaluated, showing a reduction in heteroaggregation with SiO_2 for both nanoplastic types. Sensitivity analysis indicated that the degradation half-life of the tested nanoplastics had a more significant impact on persistence than did α. The results emphasize the environmental stability of nanoplastics, particularly in freshwater and soil compartments, and the critical role of NOM and emission pathways in determining their fate.

KEYWORDS: *SimpleBox4Plastics model, plastic fate, freshwater, natural organic matter, microplastics*

INTRODUCTION

Nanoplastics (here particles with size <1 μm)[1] are formed mostly upon the degradation of plastic waste in the environment. Upon entering aquatic systems, nanoplastics may undergo alterations in their form and chemistry. These changes can include aggregation with various particulate materials in water and transformation processes such as photochemical transformation and interaction with natural organic matter (NOM), which critically influence the transport, fate, and toxicity of nanoplastics in the aquatic environment.[2] Like other nanoparticles,[3] nanoplastics may exhibit distinct behavior in achieving equilibrium partitioning compared to dissolved chemicals. Consequently, standard tests employed for determining partitioning or adsorption coefficients, such as K_{ow} and K_d, necessitate special consideration due to the potential deviation from thermodynamic expectations over varying time scales.[4]

Nanoplastics have the potential to collide with and adhere to particles of the same type, known as homoaggregation, or to particles of different types, termed heteroaggregation.[5,6] Within environmental contexts, the concentrations of nanoplastics are markedly lower than those of naturally occurring colloids such

Received: October 14, 2024
Revised: February 19, 2025
Accepted: February 20, 2025
Published: March 3, 2025

https://doi.org/10.1021/acs.est.4c10918
Environ. Sci. Technol. 2025, 59, 4674−4683

as iron oxides, silicon dioxide (SiO_2), clay minerals, etc., considering both mass and numerical aspects.[7] This increases the likelihood of nanoplastic heteroaggregation over homoaggregation in real environments. Although an increasing number of studies have been conducted in recent years to understand the heteroaggregation of nanoplastics with natural colloids,[8−10] the influence of different physicochemical parameters of nanoplastics—such as particle size and chemical composition—and environmental factors (e.g., pH, ionic strength, and NOM)[8,11] on heteroaggregation remains largely unknown. Considering the limitless number of parameter combinations that might influence the heteroaggregation of nanoplastics, it is not feasible to investigate each condition experimentally. This highlights the importance of modeling to understand the fate of heteroaggregation and subsequently of nanoplastics in the environment.

Several models have been developed to investigate the behavior of nanoparticles in the environment. Powerful tools suited for this purpose are environmental fate models such as MendNano[12] and NanoDUFLOW.[13] These models can be used to predict exposure levels and transport behavior of nanoparticles and to support a proactive risk assessment. Another model is SimpleBox4Nano (SB4N),[13] which utilizes first-order kinetics to estimate environmental background concentrations for colloids in an environmental system composed of air, soil, water, and sediment compartments represented as boxes.[13] SB4N was adapted to SimpleBox4-Plastic (SB4P), which operates on three scales: regional, continental, and global.[14] Particles within the model can exist in each compartment in three forms: freely dispersed, heteroaggregated with natural colloidal particles (<450 nm), and attached to larger particles (>450 nm).[13] The required input for SB4P can be categorized as follows: scenario settings, substance properties (e.g., attachment efficiency (α), dissolution and degradation rate constants), and emission rates. However, determining the α of nanoplastics to other colloids, which is a pivotal aspect in comprehending the characteristics of nanoplastics and their interactions within a specific system, remains challenging. In colloidal science, α is a dimensionless parameter that expresses the ratio of successful particle collisions to the total number of collisions[15] and is highlighted as a critical property for evaluating nanoparticles' fate in the environment.

Quantifying heteroaggregation and isolating individual α values from experimental data is an approach to determining α that poses significant challenges due to the multitude of concurrent competing processes of particle−particle collision.[16] Often, the methodology employed in investigating homoaggregation may not be readily adaptable to heteroaggregation, primarily due to the need to experimentally track target particles (such as engineered nanoparticles or nanoplastics) and the inherently greater complexity of the environmental system such as the presence of natural colloids and NOM which affects values of α.[17] Consequently, research on heteroaggregation remains relatively limited in comparison. Attempts have been made to adapt methods used to investigate homoaggregation to heteroaggregation, by tracking the average size evolution of aggregating particles, e.g., using dynamic light scattering (DLS).[18] However, this approach cannot differentiate particle types as needed in a study of heteroaggregation. A more general approach to quantify heteroaggregation involves measurements of individual target particles remaining in suspension over time after heteroaggregates are removed via settling[19] or filtration.[3] In the case of particles containing metals, measuring the mass or number of particles by using inductively coupled plasma mass spectrometry (ICP−MS) and single particle (sp)ICP−MS can provide information on heteroaggregation.[20,21] However, these methods face limitations when dealing with nanoplastics as they cannot be detected by ICP−MS. Recent advancements involving the entrapment of rare elements in polymeric structures have enabled the tracking of nanoplastics in such intricate environments.[6] For example, in our recent publications, we applied gadolinium (Gd) as a rare element inside polymeric particles to mimic nanoplastics and investigate the uptake of the particles by plants and their trophic transfer.[22] A previous review paper has provided detailed information about the application of this methodology for nanoplastic fate assessment.[22]

The objective of the current study is to obtain and use α values in conjunction with SB4P to understand how the variation in the chemical composition, particularly density and hydrophobicity, of nanoplastics affects their retention in different environmental compartments with their specific environmental conditions. Accordingly, we first determined the α value for heteroaggregation of PS and PVC nanoplastics with SiO_2, as a model of natural colloids, in the presence of NOM and different ionic strengths. To facilitate quantification of the nanoplastics, Gd ions are entrapped inside the nanoplastics, allowing the application of spICP-MS to measure the particle numbers over time in the experimental systems. The obtained data on the number of particles over time are used to determine α to subsequently be applied in SB4P.

METHODS AND MATERIALS

Theoretical Context. *Attachment Efficiency (α).* The theoretical context and method for α measurement using a batch test has been described in detail previously[19] and is briefly summarized here. The settling rate of individual nanoplastics is negligible due to their low density and small particle size. Instead, nanoparticles collide with natural particles, potentially leading to the attachment of the two particles and the subsequent settling of the resulting in larger aggregates.

The values of α range from 0 to 1, where $\alpha = 1$ indicates a high tendency for particles to attach to other particles or surfaces. The modified Smoluchowski equation describes the transport processes governing how nanoparticles move toward a surface and the probability of attachment following collisions between particles.[23] This equation illustrates the rate of change in the particle number concentration, which represents particles that have not undergone heteroaggregation with colloids over time. Therefore, a logarithmic plot of the initial nanoparticle concentration divided by the concentration of nanoparticles that have not formed heteroaggregates with natural colloids over time (eq 1) is expected to show a pseudo-first-order reaction. The slope of this linear relationship is anticipated to be equivalent to that of $\alpha\beta B$. In the initial phases of heteroaggregation, the breakup of the aggregate can be considered insignificant.

$$\ln\left(\frac{n\phi}{n}\right) = \alpha\beta Bt \tag{1}$$

where β is the second-order collision rate constant (volume time $^{-1}$ number $^{-1}$), B is the concentration of colloids (number

https://doi.org/10.1021/acs.est.4c10918
Environ. Sci. Technol. 2025, 59, 4674−4683

volume $^{-1}$), n is the nanoparticle number concentration per unit of volume, and $n\phi$ is the initial nanoparticle number concentration per unit volume (i.e., the concentration at time t = 0). To determine the α_{total} for any given system, $\alpha\beta B$ needs to be normalized by βB as slope $\alpha\beta Bt$ represents α at a constant value of βB. Empirically, βB can be determined by modifying the conditions of the system to eliminate barriers to attachment, where α = 1 (referred to as favorable-attachment efficiency α_{fav} = 1), while keeping the dominant nanoparticle and colloid transport mechanisms unchanged and maintaining a constant colloid concentration.[23] For instance, by increasing the ion strength of the system, using NaCl and $CaCl_2$, it is possible to achieve α_{fav} = 1. The rate constant for an α_{fav} system determined from data plotted according to eq 1 is equal to βB. Subsequently, the α_{total} for the unadjusted system can be determined by normalizing the rate constant as shown in eq 2.

$$\alpha_{total} = \frac{\alpha\beta B}{\alpha_{fav}\beta B} \quad (2)$$

Critical Coagulation Concentration (CCC). The aggregation-salt concentration plot typically demonstrates two discernible regimes: reaction-limited cluster aggregation (RLCR) and diffusion-limited cluster aggregation (DLCA) regimes. In the RLCR regime, aggregation occurs via a different mechanism. Instead of relying solely on diffusion, particles can also aggregate through specific chemical or physical interactions such as electrostatic attraction or van der Waals forces. In this regime, the rate of aggregation is determined by the frequency of encounters between particles and the likelihood that they stick together upon collision. In the DLCA regime, particles undergo random Brownian motion and aggregate when they collide and attach. This process is primarily driven by diffusion, where particles move in a fluid medium due to random motion. In this regime, the rate of aggregation is limited by diffusion of particles through the medium. The point of transition between these regimes, termed the CCC, serves as a pivotal indicator in understanding the underlying mechanisms governing nanoparticle aggregation dynamics.

Fate Factors. We utilized fate factors (FF) as an output variable, indicating the persistence of these materials in an environmental compartment and mitigating the uncertainty of emissions. These factors represent the residence time of the particles in a specific compartment. Since SB4P does not provide this directly as an output, it necessitates the calculation

$$FF_{o,c} = m_c/E_o \quad (3)$$

where $FF_{o,c}$ is the fate factor [days] for a particle in compartment c as emitted to compartment o, m_c is the output for steady-state mass [kg] for compartment c, and E_o [kg day^{-1}] is the emission of a particle emitted to compartment o: air, soil, or freshwater. This is in line with the commonly applied approach in life cycle impact assessment modeling.[24,25]

MATERIALS

The materials and chemicals used in this study were purchased from Sigma-Aldrich unless otherwise specified. Spherical PS (~250 nm) and PVC (~250 nm) were designed by our group and were custom-synthesized by cd-bioparticles (NY 11967, USA) to our specifications. The company claimed that the Gd ions are entrapped inside the particles and not on the surface. To ensure the Gd ions are inside the particles as we requested and not released from the particles during the application, we have performed a comprehensive characterization[22] (see next section). Water was deionized by reverse osmosis and further purified using a Millipore MQ system. The particles were stabilized with a Tween 20 (1%). The density of PS and PVC used in this study were 1.3−1.35 and 1.4−1.7 g cm^3, respectively, as reported by the producer due to the presence of Gd in the particles. Silicon dioxide nanoparticles of 250−300 nm were used as a model of natural colloids, which was purchased from Sigma-Aldrich. SiO_2 was purchased in powder form, and the particles were dispersed in water without any functionalization (uncovered).

Particle Characterization. The hydrodynamic size of the particles and the zeta potential (ζ) were assessed by utilizing a Zetasizer Nanodevice (Malvern Panalytical, Malvern, UK). Particle shape was determined through transmission electron microscopy (TEM) using a JEOL JEM-2100F instrument operated at 200 kV. A scanning electron microscope (Zeiss Sigma HD|VP, Carl Zeiss NTS, Cambridge, UK)-EDX was used with 4 kV for elemental mapping of the nanoplastics. To assess hydrophobicity, a droplet of particle dispersion was dried on an aluminum surface, and the contact angle was measured using Milli-Q water at room temperature, employing a KSV Cam 200 contact angle instrument. The concentration of Gd ions and the number of particles were quantified using an ICP−MS instrument (PerkinElmer NexION 350D), operating in both single-particle and standard modes.

EXPERIMENTAL SETUP FOR DETERMINING THE α

Measuring the CCC. First, we determined the CCC for the homoaggregation of the nanoplastics as well as their heteroaggregation with SiO_2. The CCC of the particles was determined by measuring their size over different $CaCl_2$ concentrations using DLS.[26] To determine the CCC for the particles upon homoaggregation, 10 mg L^{-1} PS and PVC were mixed with $CaCl_2$ concentrations of 10, 50, 100, and 1000 mM, separately. To determine the CCC for PS or PVC heteroaggregation with (10 mg L^{-1}) SiO_2, solutions of $CaCl_2$ (0.1, 1, 10, 50, 100, 150, and 200 mM) were used. The selected concentrations were chosen based on the detection limit of the DLS instrument, which is approximately 10 mg L^{-1}.[21] Accordingly, the particles were introduced into a system containing the corresponding $CaCl_2$, and their hydrodynamic sizes were promptly measured over 10 min. The obtained size was plotted over time to determine the CCC. Previous studies have shown that the fast interactions between particles and colloids are likely to occur within the first minutes.[3,23] Therefore, the 10 min duration and interval were selected to be as short as possible to ensure prompt detection after sample preparation.

Quantification of Nanoplastic Number in Different Systems. To determine α in a batch test, 200 μg L^{-1} nanoplastics (PS or PVC) were introduced into a system containing 20 mg of SiO_2 and varying concentrations of $CaCl_2$ (0.1, 1, 10, or 50 mM) in MQ water adjusted to pH 7.8 with 0.1 M NaOH. The samples were mixed by hand for 5 s in plastic tubes. The nanoplastic concentrations were chosen to establish the most environmentally relevant scenario feasible[27] while detectable with a high sensitivity. The concentration of SiO_2 was arbitrarily set to be 2 orders of magnitude higher than that of the nanoplastics. The α of nanoplastics onto SiO_2 remains independent of these initial concentrations, which demonstrates that the number concentration of SiO_2 (and its

https://doi.org/10.1021/acs.est.4c10918
Environ. Sci. Technol. 2025, 59, 4674−4683

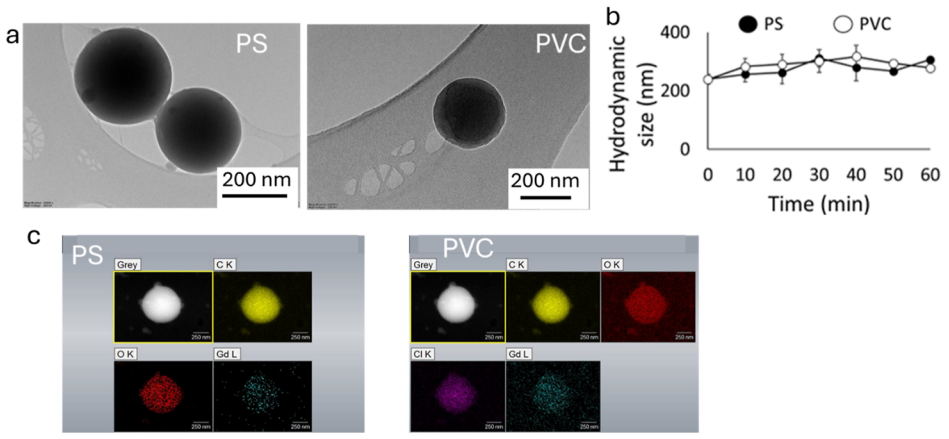

Figure 1. (a) TEM image of PS nanoplastics and PVC nanoplastics. (b) The hydrodynamic size (nm) of the particles was measured over 1 h using DLS to show the homoagglomeration profile of the particles in MQ water. (c) SEM-EDS elemental mapping of PS (the particles, carbon, oxygen, and Gd) and PVC (the particles, carbon, oxygen, chlorine, and Gd) nanoplastics showing the distribution of Gd in the particles.

associated available surface area) is substantially higher than that of the nanoplastics.[3] The selection of Ca^{2+} and their ranges was guided by OECD test number 318.[28] Divalent ions like Ca^{2+} are commonly found at concentrations capable of influencing colloidal stability.[29] To determine the influence of NOM on heteroaggregation of nanoplastics and SiO_2, nanoplastics were introduced in a system containing 20 mg of SiO_2, 10 mM $CaCl_2$, and 50 mg L^{-1} dissolved NOM. The NOM was collected from the Hietajarvi S catchment area in Finland and dissolved according to the following method.[29] This concentration of NOM was selected to represent the average to high concentrations of NOM in natural freshwater of the EU.[29] A minimum of five replicate tests were conducted for each system. The setup of the spICP-MS is given in the Supporting Information (Table S1).

Calculating Attachment Efficiency (α). The measured number concentration of the nanoplastics was plotted against the aggregation time (minutes), generating a removal curve for the particles in each system. We calculated both Ct_0/Ct and ln (Ct_0/Ct) for the initial 5 data points, where Ct_0 represents the particle count at time 0 and Ct represents the particle count at the specified time (t). The natural logarithm of the first five data points was plotted as a function of time to linearize the removal curves (pseudo-first-order kinetics).[23] A fundamental assumption is that during the initial attachment phase (first five data points), the occurrence of breakup of the heteroaggregates is negligible. We calculated the slope of a regression line through the linear portion, which represents the quantity mM βB (eq 2) for nanoplastics with the SiO_2 colloids. We selected these time points to be included in the linear regression because (1) the attachment period commences at the first measured time point, (2) it encompasses three or more consecutive points, and (3) it yields the highest coefficient of determination (R^2).[23] We determine the value of α for each system by using the obtained value of $\alpha\beta B$ in eq 2, the known concentration of SiO_2 colloids, and normalizing it by the slope for favored heteroaggregation at the CCC, where α is 1.

Simple Box Model. In this study, we applied SimpleBox4-Plastics (v4.04)[30] as earlier described by Quik et al.,[14] for the calculation of FF. To compare the effect of the calculated α and other variables related to the characteristics of the particles, these are applied probabilistically to determine their effect on the persistence of these particles in air, water, sediment, and soil. All input variables, not related to the characteristics of the particles, are taken deterministically using the default values already present in SB4P. The probabilistic calculations were performed using the @Risk Excel plugin (v8, Palisade) following the distribution given in the Supporting Information (Section 2). These include variations in size and density and uncertainty in the degradation and fragmentation rate constants in addition to the range in attachment efficiencies based on the measurements reported here. Both uniform and triangular distributions were used. A uniform distribution is used when it is expected that the values vary equally between a minimum and a maximum. A triangular distribution is used when values vary normally around a top value, i.e., the most likely value. This is preferred over normal distribution, to prevent extreme values from having a disproportionate impact. Furthermore, 10,000 iterations were performed. The air, freshwater + sediment, soil, and seawater + sediment compartments are considered for a scenario at the continental scale. Emissions are considered to be in air, freshwater, and soil. The subcompartments from soil (e.g., agricultural, natural, other soil) and freshwater (e.g., lake and river) are not separately considered to produce concise results. This means that three emission routes lead to different environmental compartments resulting in a total of 17 FF (see Table S2). These FFs are not just one value, considering the 10,000 possible interactions. Further details on model parameterization are reported in the Supporting Information (Section 2).

Data Analysis. Here we used @Risk to probabilistically run the latest SB4P model according to the method reported previously.[14] The graphs were plotted using Microsoft Office 2022 and R (v.4.3.1) (https://www.R-project.org/). Statistical evaluation of the data for normality was conducted utilizing a Shapiro–Wilk test through IBM SPSS statistics 29.0.2.

RESULTS AND DISCUSSION

Particle Characterization. The spherical pristine PS and PVC nanoplastics were thoroughly characterized by using DLS and spICP-MS (Figure 1). The nominal particle diameters for PS and PVC were both 250 nm, with polydispersity indices (PDI) of 0.1 and 0.2, respectively. Analysis using DLS revealed hydrodynamic diameters consistent with nominal sizes, corroborated by TEM observations based on the average size of 100 particles per nanoplastic type, indicating a uniform size

https://doi.org/10.1021/acs.est.4c10918
Environ. Sci. Technol. 2025, 59, 4674−4683

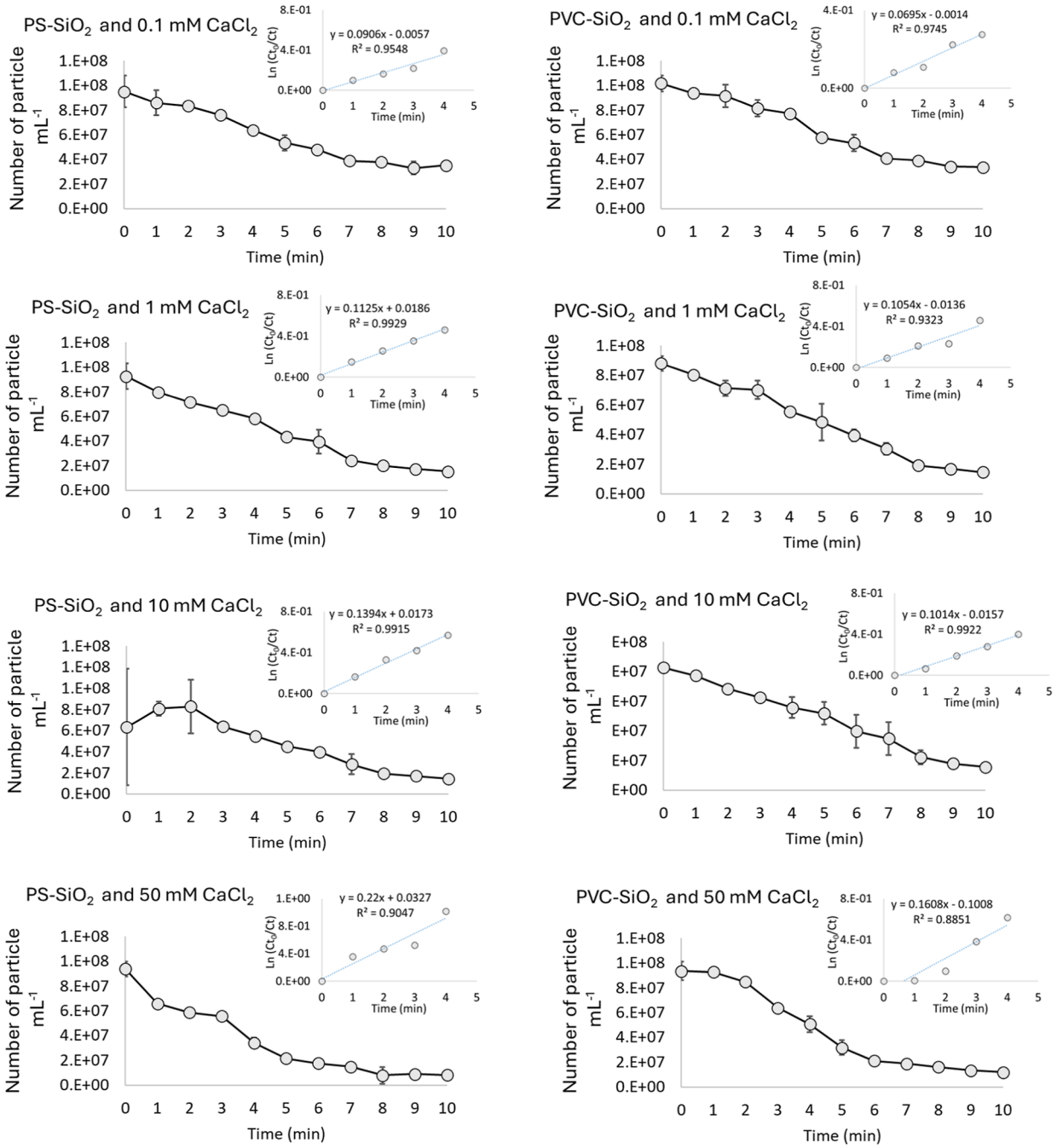

Figure 2. Number of PS and PVC nanoplastics in the presence of SiO_2 and varying ionic strengths were measured using spICP-MS over 10 min. The results show the mean ± standard deviation. Calculated (Ct_0/Ct) and the natural logarithm of (Ct_0/Ct) for the first five data points are shown in the smaller graphs.

distribution (Figure 1a,b) for the nanoplastics and SiO_2. The TEM image further confirmed that the SiO_2 particles (Figure S1) used in this study exhibited a spherical morphology with an approximate size of 250 nm, matching the dimensions of the nanoplastics. PS nanoplastics exhibited a contact angle of 80 ± 2°, signifying higher hydrophobicity compared to PVC nanoplastics with a contact angle of 60 ± 1°. Furthermore, ζ measurements conducted in Milli-Q water indicated a negative charge for PS (−46 ± 2 mV), PVC (−48 ± 1 mV), and SiO_2 (−27 ± 4 mV) particles. This negative ζ suggests a propensity for particle−particle repulsion, minimizing agglomeration tendencies.[27]

Particle Stability. To perform an aggregation-related study using nanoparticles, it is important to ensure the stability of the pristine particles against aggregation and transformation to prevent uncontrolled changes in the particles.[29] Investigation of nanoplastics' stability in the context of homoaggregation involved monitoring hydrodynamic sizes using DLS over a 1 h duration (Figure 1b). The size of the particles did not increase significantly over time, indicating stability against homoaggregation. To ensure that the detectable Gd quantity within the particles using spICP-MS is representative of the number of particles, we conducted a comparison between the number of nanoplastics measured by spICP-MS and both the nominal concentration and particle count measured by DLS. Our

https://doi.org/10.1021/acs.est.4c10918
Environ. Sci. Technol. 2025, 59, 4674−4683

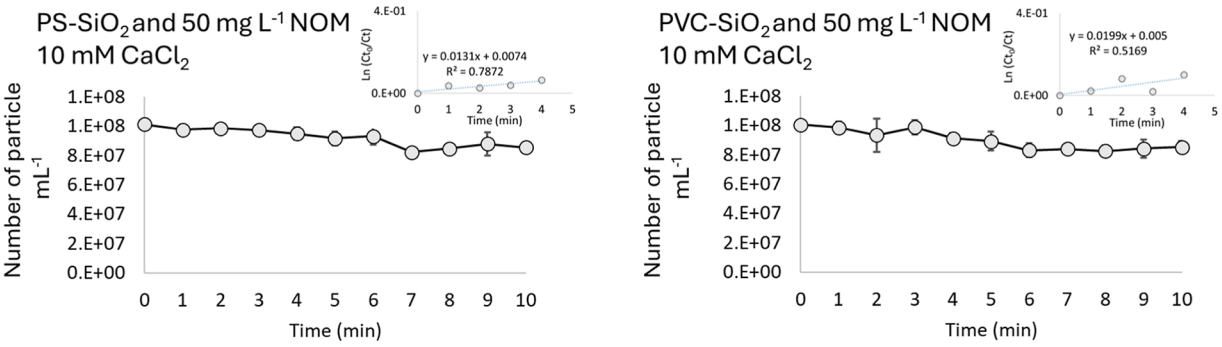

Figure 3. Number of PS and PVC nanoplastics in the presence of SiO_2, 50 mg L^{-1} NOM, and 10 mM $CaCl_2$ over 10 min of mixing time. The results show the mean ± standard deviation. The calculated (Ct_0/Ct) and the natural logarithm of (Ct_0/Ct) for the first five data points are shown in the smaller graphs.

results revealed statistically insignificant differences in the number of nanoplastics measured by the different techniques for both particle types (Figure S2).

Scanning electron microscopy (SEM) images coupled with energy-dispersive spectroscopy (EDS) analysis depicted the elemental distribution of Gd within PS and PVC nanoplastics (Figure 1c). It is noteworthy that the Gd ions were entrapped within the particles rather than being present on their surface. The Gd content within the particles was quantified to be 9.7%−11%.[22] To ensure the retention of Gd within the particles and prevent leaching, we initially assessed particle stability by examining Gd ions in the nanoplastics dispersion in MQ water following a 72 h mixing at room temperature using spICP-MS. Importantly, no Gd ions were detectable in the supernatants, indicating robust particle stability and minimal leaching.

Homo- and Heteroaggregation. First, we determined the CCC values of PS and PVC nanoplastics in different $CaCl_2$ concentrations using DLS. The CCC values for both particles were not found even in a ∼1000 mM $CaCl_2$ solution, indicating the stability of the particles against homoaggregation. The measured ζ values are reported in Table S3. Then, we measured the CCC for PS and PVC nanoplastics in combination with SiO_2 particles (PS−SiO_2 and PVC−SiO_2) in a $CaCl_2$ solution, which was ∼100 mM. At this $CaCl_2$ concentration, the α is assumed to be 1 (favorable attachment, $\alpha = 1$).[19]

The number of nanoplastics (PS or PVC) in the medium with 20 mg L^{-1} SiO_2 and different concentrations of $CaCl_2$ was measured using spICP-MS for 10 min. As shown in Figure 2, the number of PS and PVC nanoplastics decreased in the supernatant over time, indicating the removal of particles from the dispersion phase. Considering that homoaggregation of PS−PS and PVC−PVC in the dispersion is not occurring due to the stability of the particles in this $CaCl_2$ solution against homoaggregation, the only explanation for the decreased concentration of the nanoplastics is heteroaggregation of the particles with SiO_2. A previous study showed that the CCC of 2 mM L^{-1} for both $CaCl_2$ and $MgCl_2$ was reached for fragmental PET particles, suggesting that in freshwater, nanoplastics are likely to aggregate rapidly under more alkaline conditions.[31] The highest aggregation rate is expected in marine water due to the combination of high ionic strength (≈0.7 M L^{-1}), a high concentration of multivalent ions (e.g., Ca^{2+}, Mg^{2+}), and low NOM content. We determined (Ct_0/Ct) and the natural logarithm of (Ct_0/Ct) for the first five data points (Figure 2), where Ct_0 is the number of particles at time 0 and Ct is the number of particles at the time of interest. The graph of the first five data points was plotted because the coefficient of determination (R^2) was higher than 90%. Removal curves for all systems followed pseudo-first-order kinetics, allowing for linear regression, assuming that newly formed heteroaggregates did not break up.

We measured the heteroaggregation of PS and PVC with SiO_2 in the presence of the NOM and $CalC_2$. Accordingly, the number of nanoplastics in the dispersion of NOM (50 mg L^{-1}), SiO_2 (20 mg L^{-1}), and $CaCl_2$ (10 mM) was measured over 10 min (Figure 3). The results showed that the presence of NOM minimized the observed decreases in the numbers of both nanoplastics (PS and PVC) in the dispersion, even in the presence of 100 mM $CaCl_2$. This suggests that NOM can stabilize SiO_2 and subsequently decrease the heteroaggregation between them and the nanoplastics, similar to what has been reported for metallic nanoparticles.[17] Alimi et al.[26] reported that, in the absence of NOM, the CCC of PS nanoplastics in $CaCl_2$ was independent of particle size. The addition of humic acid enhanced aggregation via bridging, regardless of the size of the plastics, while fulvic acid had little to no effect. In the NOM, alginate stabilized the particle suspensions. The composition of the used NOM in this study was described previously.[32] The adsorption of NOM to the surface of nanoplastics and SiO_2 can lead to steric repulsion between the particles, where the NOM molecules form a protective layer that prevents close interaction and aggregation.[33] This phenomenon is significant in aquatic environments, where NOM concentrations and qualities vary widely and influence the dispersion and stability of nanoplastics.

Calculated Attachment Efficiency for Different Water Conditions. We calculated the α from the particle removal results using eq 2. The results (Table 1) showed that α for PS−SiO_2 was slightly higher than that for PVC−SiO_2. Indeed, the observed differences in α between PS−SiO_2 and PVC−SiO_2 despite identical size and shape of PS and PVC nanoplastics likely stem from variations in other physicochemical properties, e.g., density and hydrophobicity. Differences in density affect the buoyancy and settling rates of nanoplastics in a suspension. Higher-density particles may settle more quickly, influencing the observed aggregation rates. Additionally, denser particles might interact differently with other particles or with the surrounding medium, affecting the aggregation behavior. More hydrophobic particles are likely to aggregate more readily due to stronger van der Waals forces and reduced repulsion between particles. Hydrophobic interactions can lead to increased clustering and aggregation, especially in non-

https://doi.org/10.1021/acs.est.4c10918
Environ. Sci. Technol. 2025, 59, 4674−4683

Table 1. Calculated α for Nanoplastics of Different Chemical Compositions and SiO_2 under Different Water Conditions[a]

nanoplastics-SiO_2	water condition: pH: 8, MQ water	α_{global}
PS−SiO_2	0.1 mM $CaCl_2$	0.24 ± 0.03
	1 mM $CaCl_2$	0.31 ± 0.051
	10 mM $CaCl_2$	0.37 ± 0.05
	50 mM $CaCl_2$	0.6 ± 0.08
	50 mg L^{-1} NOM, 10 mM $CaCl_2$	0.03 ± 0.001
PVC−SiO_2	0.1 mM $CaCl_2$	0.34 ± 0.04
	1 mM $CaCl_2$	0.5 ± 0.07
	10 mM $CaCl_2$	0.5 ± 0.06
	50 mM $CaCl_2$	0.8 ± 0.07
	50 mg L^{-1} NOM, 10 mM $CaCl_2$	0.05 ± 0.001

[a]NOM: natural organic matter.

aqueous environments or in the presence of hydrophobic substances. These variations can influence the surface properties, and interaction potentials of the tested nanoparticles with SiO_2, thereby impacting their α under changing ionic strength conditions. However, it was observed that α values of nanoplastics and SiO_2 decreased with increasing concentrations of $CaCl_2$ for both PS and PVC particles. This outcome was anticipated as an elevation in ionic strength (i.e., $CaCl_2$) is known to contract the electrical double layer surrounding the particles, thereby promoting heteroaggregation between nanoplastics and SiO_2 because of the attraction generated by van der Waals forces.[8,34]

The introduction of 50 mg L^{-1} NOM resulted in a decrease in α even in the presence of 10 mM $CaCl_2$. NOM, a complex mixture of organic compounds derived from the degradation of plant and animal materials such as humic and fulvic acids, can attach to the surface of SiO_2 and nanoplastics.[8] The presence of NOM on particle surfaces can induce repulsion among the particles.[33] Consequently, this repulsion effect diminishes the likelihood of particle attachment, thereby reducing α and minimizing the formation of heteroaggregation.

Fate Model Output Analysis. Uncertainties in particle characteristics, such as size, density, attachment efficiency, and degradation half-life, were incorporated into the SB4P model. This study marks the first exact measurements of α for nanoplastics. Surprisingly, the results indicate that variations in α, especially in scenarios with and without dissolved NOM, do not significantly affect FF. It is assumed that natural waters typically contain some level of often very heterogeneous NOM, suggesting that attachment efficiencies likely range between 0.01 and 1 depending on the NOM concentration and type as well as water salinity. Despite these ranges, no substantial impact on the FF was observed, as shown in Figure 4.

However, the degradation half-life of PS and PVC emerged as a more critical factor, significantly influencing the persistence of PVC and PS in the environment. Although these were not measured for PVC and PS specifically, roughly

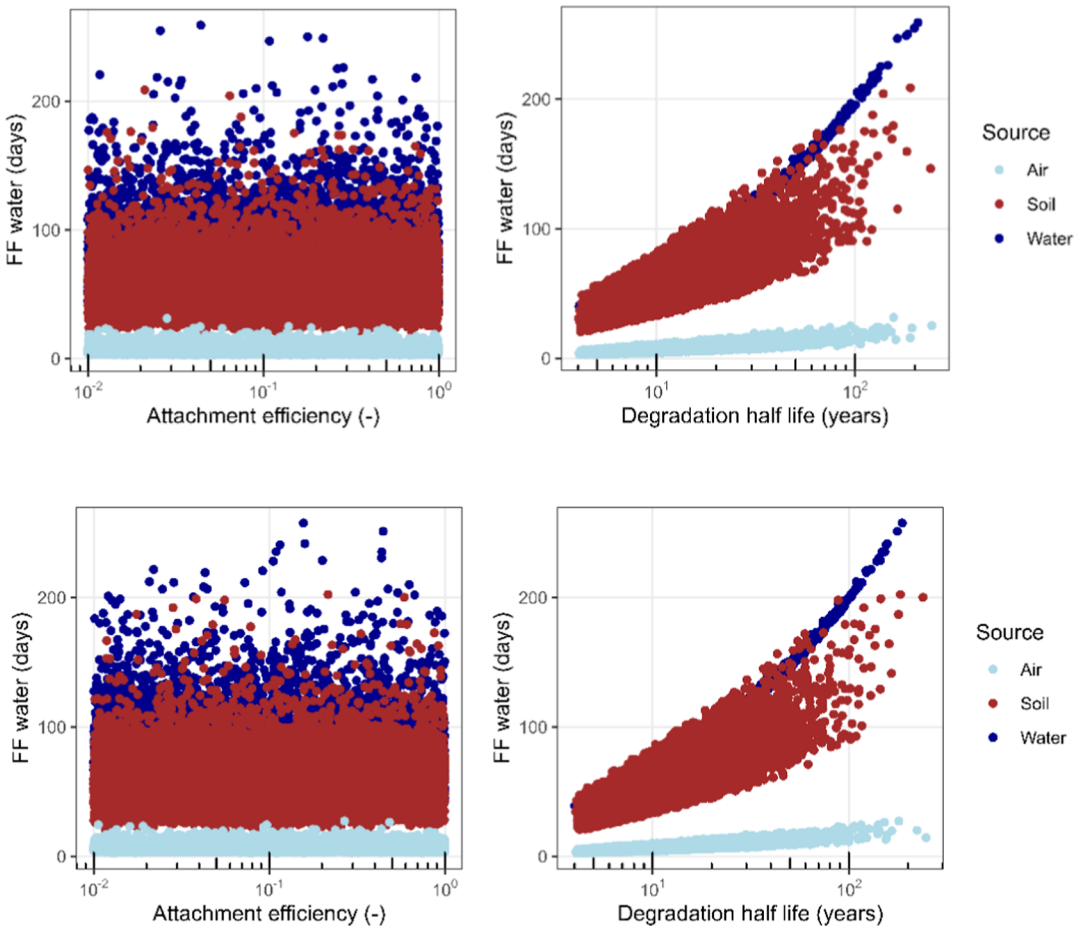

Figure 4. Fate factors for freshwater versus variability in attachment efficiency and soil/sediment degradation half-life for PVC (top) and PS (bottom). The rest of the figures are provided in the Supporting Information, Figures S3−S8.

https://doi.org/10.1021/acs.est.4c10918
Environ. Sci. Technol. 2025, 59, 4674−4683

Table 2. Average Fate Factors (FF) Calculated per Source Route and Environmental Compartment[a]

source	nanoplastic	N	air	freshwater sediment	freshwater	marine sediment	seawater	soil
air	PS	10,000	5.30	1.24	7.10	0.23	36.09	8.56
air	PVC	10,000	5.25	1.58	7.47	0.26	35.99	9.19
soil	PS	10,000	na	10.09	58.21	0.23	46.36	123.42
soil	PVC	10,000	na	12.15	57.61	0.28	45.70	122.70
water	PS	10,000	na	105.08	76.76	1.14	54.28	na
water	PVC	10,000	na	106.53	76.10	1.18	53.59	na

[a]na: not available, indicating model output is 0 kg in these compartments resulting in a FF of 0.

3 orders of magnitude range are taken, based on earlier estimates,[14] compared to only two for the α. Nevertheless, a clear relationship was seen, with almost all of the variability for FF in soil and sediment related to the degradation half-life in those compartments. This is in line with an earlier environmental fate modeling study on metallic nanoparticles[12] where the predicted environmental concentration was sensitive to degradation half-life, which was larger than 0.5 years, and attachment efficiencies lower than 10^{-4}. It remains to be determined whether other environmental factors, such as pH, could further reduce α to such low values. The data presented suggest that in the presence of NOM, the α decreases by about 1 order of magnitude. It is important to note that the model scenario does not account for all local variability in terrestrial and aquatic systems. Additionally, using SiO_2 as a model simplifies the complexity of natural suspended particulate matter (SPM) and other colloids present in the environment. However, given the ubiquity of SiO_2 particles, the concentration and number of particles per unit surface area of SPM and natural colloids are likely to influence heteroagglomeration more significantly than the type of particle itself.

Furthermore, the calculated FF indicates that the highest values are observed for PVC and PS ending up in soil and freshwater sediment compartments (Table 2). The emission route significantly influences these outcomes; emissions to soil result in the majority of PVC and PS being retained in the soil compartment, whereas emissions to water lead to accumulation primarily in freshwater sediment. Specifically, for both PS and PVC particles emitted to air, significant amounts are found in seawater, followed by soil and air compartments. When emitted to the soil, both PS and PVC exhibit substantial retention in soil and freshwater sediment compartments regardless of emission pathways. Conversely, particles emitted directly into water predominantly accumulate in freshwater sediment. These findings underscore the importance of emission pathways in determining the environmental distribution and fate of nanoplastics like PS and PVC, highlighting potential ecological implications across different environmental compartments.

Our study provides critical insights into the aggregation kinetics and environmental fate of PS and PVC nanoplastics. The experimental findings demonstrated that nanoplastics are highly stable against homoaggregation but prone to heteroaggregation with SiO_2 under high ionic strength. The presence of NOM significantly reduces the level of aggregation, highlighting its role in stabilizing nanoplastics in natural waters. Importantly, our fate modeling showed that degradation half-life, rather than attachment efficiency, is the primary factor influencing the persistence of nanoplastics in the environment, particularly in soil and freshwater sediments. These findings underscore the necessity of considering both chemical and environmental factors such as NOM and ionic strength when predicting the fate of nanoplastics. This research advances the understanding of nanoplastic behavior and highlights the need for further investigation into their long-term ecological impact across different environmental compartments.

The high stability of PS and PVC nanoplastics against homoaggregation suggests prolonged dispersion in natural waters, potentially increasing their bioavailability to aquatic organisms. The observed heteroaggregation with SiO_2 under high ionic strength conditions indicates that nanoplastics may settle into sediments of marine environments, posing long-term risks to benthic ecosystems. Furthermore, the reduction in aggregation due to NOM suggests that nanoplastics may remain suspended for longer periods in water bodies rich in organic material, enhancing their transport over long distances and increasing the risk of incorporation by organisms such as plants and animals, and thus the health risk for humans.

The fate modeling results highlight that nanoplastics emitted into air, freshwater, or soil predominantly accumulate in soil and sediment compartments, raising concerns about their persistence in terrestrial and aquatic environments. The significant influence of the degradation half-life on the fate of these particles underscores the need for accurate degradation rates in environmental risk assessments. These findings stress the potential for nanoplastics to act as long-term environmental contaminants, necessitating the development of targeted mitigation strategies to reduce their release and enhance their degradation in natural ecosystems. The role of emission pathways in determining their environmental distribution also suggests that regulations should focus on minimizing plastic emissions, particularly in regions with vulnerable ecosystems.

■ ASSOCIATED CONTENT

Supporting Information

The Supporting Information is available free of charge at https://pubs.acs.org/doi/10.1021/acs.est.4c10918.

spICP-MS settings, including radio frequency power, gas flows, dwell time, and acquisition time, ensuring precise nanoplastic characterization; EUSES settings in SB4P used for model parameterization to simulate the fate and transport of PS and PVC nanoplastics; experimentally determined substance properties, such as particle radii, density, and Hamaker constants incorporated into the model using triangular or uniform distributions; attachment efficiencies and degradation rates parameterized using data from experiments under varying environmental conditions; and detailed overview of the parameters, distributions, and fate factor calculations supporting the analysis (PDF)

https://doi.org/10.1021/acs.est.4c10918
Environ. Sci. Technol. 2025, 59, 4674−4683

AUTHOR INFORMATION

Corresponding Author

Fazel Abdolahpur Monikh − *Department of Chemical Sciences, University of Padua, 35122 Padua, Italy; Department of Environmental and Biological Sciences, University of Eastern Finland, 80101 Joensuu, Finland; Institute for Nanomaterials, Advanced Technologies, and Innovation, Technical University of Liberec Bendlova 1409/7, 460 01 Liberec, Czech Republic;* orcid.org/0000-0001-9500-5303; Email: Fazel.Monikh@unipd.it

Authors

Joris T. K. Quik − *National Institute for Public Health and Environment (RIVM), Centre for Sustainability, Health and Environment, 3721 MA Bilthoven, The Netherlands;* orcid.org/0000-0002-7964-3652

Mark R. Wiesner − *Department of Civil and Environmental Engineering, Duke University, Durham, North Carolina 27708, United States; Center for the Environmental Implications of NanoTechnology (CEINT), Duke University, Durham, North Carolina 27708, United States;* orcid.org/0000-0002-0823-5045

Andrea Tapparo − *Department of Chemical Sciences, University of Padua, 35122 Padua, Italy;* orcid.org/0000-0001-8928-705X

Paolo Pastore − *Department of Chemical Sciences, University of Padua, 35122 Padua, Italy;* orcid.org/0000-0003-1448-0175

Hans-Peter Grossart − *Department of Plankton and Microbial Ecology, Leibniz Institute for Freshwater Ecology and Inland Fisheries, 16775 Berlin, Germany; Institute of Biochemistry and Biology, Potsdam University, 14469 Potsdam, Germany;* orcid.org/0000-0002-9141-0325

Jarkko Akkanen − *Department of Environmental and Biological Sciences, University of Eastern Finland, 80101 Joensuu, Finland;* orcid.org/0000-0001-9232-0121

Raine Kortet − *Department of Environmental and Biological Sciences, University of Eastern Finland, 80101 Joensuu, Finland*

Jussi V.K. Kukkonen − *Department of Environmental and Biological Sciences, University of Eastern Finland, 80101 Joensuu, Finland; Department of Environmental and Biological Sciences, University of Eastern Finland, Kuopio 70211, Finland*

Complete contact information is available at: https://pubs.acs.org/10.1021/acs.est.4c10918

Notes

The authors declare no competing financial interest.

ACKNOWLEDGMENTS

The authors acknowledge funding from the European Union's Horizon 2020 Research and Innovation programme, under the Grant Agreement number 965367 (PlasticsFatE). This project was also supported by Research project P-DiSC-2023 University of Padua, Research Council of Finland project 362379, and the UEF Water program. The authors thank Rolf Vogt, Dag Olav Andersen, and the Natural Organic Matter in the Nordic Countries project for providing the NOM isolate.

REFERENCES

(1) Abdolahpur Monikh, F.; Hansen, S. F.; Vijver, M.; Kentin, E.; Nielsen, M. B.; Baun, A.; Syberg, K.; Lynch, I.; Valsami-Jones, E.; Peijnenburg, W. Can Current Regulations Account for Intentionally Produced Nanoplastics? *Environ. Sci. Technol.* **2022**, *56* (7), 3836−3839.

(2) Meng, Z.; Recoura-Massaquant, R.; Chaumot, A.; Stoll, S.; Liu, W. Acute Toxicity of Nanoplastics on Daphnia and Gammarus Neonates: Effects of Surface Charge, Heteroaggregation, and Water Properties. *Sci. Total Environ.* **2023**, *854*, 158763.

(3) Geitner, N. K.; O'Brien, N. J.; Turner, A. A.; Cummins, E. J.; Wiesner, M. R. Measuring Nanoparticle Attachment Efficiency in Complex Systems. *Environ. Sci. Technol.* **2017**, *51* (22), 13288−13294.

(4) Praetorius, A.; Tufenkji, N.; Goss, K.-U.; Scheringer, M.; von der Kammer, F.; Elimelech, M. The Road to Nowhere: Equilibrium Partition Coefficients for Nanoparticles. *Environ. Sci.:Nano* **2014**, *1* (4), 317.

(5) Lagarde, F.; Olivier, O.; Zanella, M.; Daniel, P.; Hiard, S.; Caruso, A. Microplastic Interactions with Freshwater Microalgae: Hetero-Aggregation and Changes in Plastic Density Appear Strongly Dependent on Polymer Type. *Environ. Pollut.* **2016**, *215*, 331−339.

(6) Abdolahpur Monikh, F.; Vijver, M. G.; Mitrano, D. M.; Leslie, H. A.; Guo, Z.; Zhang, P.; Lynch, I.; Valsami-Jones, E.; Peijnenburg, W. J. G. M. The Analytical Quest for Sub-Micron Plastics in Biological Matrices. *Nano Today* **2021**, *41*, 101296.

(7) Pradel, A.; Ferreres, S.; Veclin, C.; El Hadri, H.; Gautier, M.; Grassl, B.; Gigault, J. Stabilization of Fragmental Polystyrene Nanoplastic by Natural Organic Matter: Insight into Mechanisms. *ACS ES&T Water* **2021**, *1* (5), 1198−1208.

(8) Oriekhova, O.; Stoll, S. Heteroaggregation of Nanoplastic Particles in the Presence of Inorganic Colloids and Natural Organic Matter. *Environ. Sci.:Nano* **2018**, *5* (3), 792−799.

(9) Wu, J.; Liu, J.; Wu, P.; Sun, L.; Chen, M.; Shang, Z.; Ye, Q.; Zhu, N. The Heteroaggregation and Deposition Behavior of Nanoplastics on Al2O3 in Aquatic Environments. *J. Hazard. Mater.* **2022**, *435*, 128964.

(10) Wu, J.; Ye, Q.; Wu, P.; Xu, S.; Liu, Y.; Ahmed, Z.; Rehman, S.; Zhu, N. Heteroaggregation of Nanoplastics with Oppositely Charged Minerals in Aquatic Environment: Experimental and Theoretical Calculation Study. *Chem. Eng. J.* **2022**, *428*, 131191.

(11) Wu, J.; Ye, Q.; Li, P.; Sun, L.; Huang, M.; Liu, J.; Ahmed, Z.; Wu, P. The Heteroaggregation Behavior of Nanoplastics on Goethite: Effects of Surface Functionalization and Solution Chemistry. *Sci. Total Environ.* **2023**, *870*, 161787.

(12) Meesters, J. A. J.; Peijnenburg, W. J. G. M.; Hendriks, A. J.; Van De Meent, D.; Quik, J. T. K. A Model Sensitivity Analysis to Determine the Most Important Physicochemical Properties Driving Environmental Fate and Exposure of Engineered Nanoparticles. *Environ. Sci.:Nano* **2019**, *6* (7), 2049−2060.

(13) Meesters, J. A. J.; Koelmans, A. A.; Quik, J. T. K.; Hendriks, A. J.; Van De Meent, D. Multimedia Modeling of Engineered Nanoparticles with SimpleBox4nano: Model Definition and Evaluation. *Environ. Sci. Technol.* **2014**, *48* (10), 5726−5736.

(14) Quik, J. T. K.; Meesters, J. A. J.; Koelmans, A. A. A Multimedia Model to Estimate the Environmental Fate of Microplastic Particles. *Sci. Total Environ.* **2023**, *882*, 163437.

(15) Zhang, W.; Crittenden, J.; Li, K.; Chen, Y. Attachment Efficiency of Nanoparticle Aggregation in Aqueous Dispersions: Modeling and Experimental Validation. *Environ. Sci. Technol.* **2012**, *46* (13), 7054−7062.

(16) Praetorius, A.; Badetti, E.; Brunelli, A.; Clavier, A.; Gallego-Urrea, J. A.; Gondikas, A.; Hassellöv, M.; Hofmann, T.; Mackevica, A.; Marcomini, A.; Peijnenburg, W.; Quik, J. T. K.; Seijo, M.; Stoll, S.; Tepe, N.; Walch, H.; Von Der Kammer, F. Strategies for Determining Heteroaggregation Attachment Efficiencies of Engineered Nanoparticles in Aquatic Environments. *Environ. Sci.:Nano* **2020**, *7* (2), 351−367.

(17) Clavier, A.; Praetorius, A.; Stoll, S. Determination of Nanoparticle Heteroaggregation Attachment Efficiencies and Rates in Presence of Natural Organic Matter Monomers. Monte Carlo Modelling. *Sci. Total Environ.* **2019**, *650*, 530−540.
(18) Hou, J.; Ci, H.; Wang, P.; Wang, C.; Lv, B.; Miao, L.; You, G. Nanoparticle Tracking Analysis versus Dynamic Light Scattering: Case Study on the Effect of Ca2+ and Alginate on the Aggregation of Cerium Oxide Nanoparticles. *J. Hazard. Mater.* **2018**, *360*, 319−328.
(19) Barton, L. E.; Therezien, M.; Auffan, M.; Bottero, J. Y.; Wiesner, M. R. Theory and Methodology for Determining Nanoparticle Affinity for Heteroaggregation in Environmental Matrices Using Batch Measurements. *Environ. Eng. Sci.* **2014**, *31* (7), 421−427.
(20) Abdolahpur Monikh, F.; Chupani, L.; Vijver, M. G.; Vancová, M.; Peijnenburg, W. J. G. M. Analytical Approaches for Characterizing and Quantifying Engineered Nanoparticles in Biological Matrices from an (Eco)Toxicological Perspective: Old Challenges, New Methods and Techniques. *Sci. Total Environ.* **2019**, *660*, 1283−1293.
(21) Abdolahpur Monikh, F.; Guo, Z.; Zhang, P.; Vijver, M. G.; Lynch, I.; Valsami-Jones, E.; Peijnenburg, W. J. G. M. An Analytical Workflow for Dynamic Characterization and Quantification of Metal-Bearing Nanomaterials in Biological Matrices. *Nat. Protoc.* **2022**, *17* (9), 1926−1952.
(22) Abdolahpur Monikh, F.; Holm, S.; Kortet, R.; Bandekar, M.; Kekäläinen, J.; Koistinen, A.; Leskinen, J. T. T.; Akkanen, J.; Huuskonen, H.; Valtonen, A.; Dupuis, L.; Peijnenburg, W.; Lynch, I.; Valsami-Jones, E.; Kukkonen, J. V. K. Quantifying the Trophic Transfer of Sub-Micron Plastics in an Assembled Food Chain. *Nano Today* **2022**, *46*, 101611.
(23) Turner, A. A.; Rogers, N. M. K.; Wiesner, M. R.; Geitner, N. K. Nanoparticle Affinity for Natural Soils: A Functional Assay for Determining Particle Attachment Efficiency in Complex Systems. *Environ. Sci.:Nano* **2020**, *7* (6), 1719−1729.
(24) Ettrup, K.; Kounina, A.; Hansen, S. F.; Meesters, J. A. J.; Vea, E. B.; Laurent, A. Development of Comparative Toxicity Potentials of TiO2 Nanoparticles for Use in Life Cycle Assessment. *Environ. Sci. Technol.* **2017**, *51* (7), 4027−4037.
(25) Salieri, B.; Hischier, R.; Quik, J. T. K.; Jolliet, O. Fate Modelling of Nanoparticle Releases in LCA: An Integrative Approach towards "USEtox4Nano. *J. Cleaner Prod.* **2019**, *206*, 701−712.
(26) Alimi, O. S.; Farner, J. M.; Rowenczyk, L.; Petosa, A. R.; Claveau-Mallet, D.; Hernandez, L. M.; Wilkinson, K. J.; Tufenkji, N. Mechanistic Understanding of the Aggregation Kinetics of Nanoplastics in Marine Environments: Comparing Synthetic and Natural Water Matrices. *J. Hazard. Mater. Adv.* **2022**, *7* (June), 100115.
(27) Bandekar, M.; Abdolahpur Monikh, F.; Kekäläinen, J.; Tahvanainen, T.; Kortet, R.; Zhang, P.; Guo, Z.; Akkanen, J.; Leskinen, J. T. T.; Gomez-Gonzalez, M. A.; Krishna Darbha, G.; Grossart, H. P.; Valsami-Jones, E.; Kukkonen, J. V. K. Submicron Plastic Adsorption by Peat, Accumulation in Sphagnum Mosses and Influence on Bacterial Communities in Peatland Ecosystems. *Environ. Sci. Technol.* **2022**, *56* (22), 15661−15671.
(28) Organization for Economic Cooperation and Development. *GD 318: Guidance Document for the Testing of Dissolution and Dispersion Stability of Nanomaterials and the Use of the Data for Further Environmental Testing and Assessment Strategies. Series on Testing and Assessment No. 318*. OECD Guidel. Test. Chem. 2020.
(29) Abdolahpur Monikh, F.; Praetorius, A.; Schmid, A.; Kozin, P.; Meisterjahn, B.; Makarova, E.; Hofmann, T.; von der Kammer, F. Scientific Rationale for the Development of an OECD Test Guideline on Engineered Nanomaterial Stability. *NanoImpact* **2018**, *11*, 42−50.
(30) Quik, J. *Rivm-Syso/SimpleBox: SimpleBox4plastic Xl4plastic_v4.0.4*; Zenodo, 2024.
(31) Dong, S.; Cai, W.; Xia, J.; Sheng, L.; Wang, W.; Liu, H. Aggregation Kinetics of Fragmental PET Nanoplastics in Aqueous Environment: Complex Roles of Electrolytes, PH and Humic Acid. *Environ. Pollut.* **2021**, *268*, 115828.
(32) Chatterjee, B.; Gjessing, E.; Kukkonen, J. V. K.; Larsen, H. E.; Luster, J.; Paul, A.; Pflugmacher, S.; Starr, M.; Steinberg, C. E. W.; Schmitt-Kopplin, P.; Vogt, R. D.; Akkanen, J.; Andersen, D. O.; Zsolnay, A. -.; Brüggemann, R. Key site variables governing the functional characteristics of Dissolved Natural Organic Matter (DNOM) in Nordic forested catchments. *Aquat. Sci.* **2004**, *66*, 195−210.
(33) Wang, Z.; Zhang, L.; Zhao, J.; Xing, B. Environmental Processes and Toxicity of Metallic Nanoparticles in Aquatic Systems as Affected by Natural Organic Matter. *Environ. Sci.: Nano* **2016**, *3*, 240−255.
(34) Pradel, A.; Catrouillet, C.; Gigault, J. The Environmental Fate of Nanoplastics: What We Know and What We Need to Know about Aggregation. *NanoImpact* **2023**, *29*, 100453.

https://doi.org/10.1021/acs.est.4c10918
Environ. Sci. Technol. 2025, 59, 4674−4683